The unitarity problem in the theory of the Froissaron exchange

M. S. Dubovikov

Institute of Theoretical and Experimental Physics

K. A. Ter Martirosyan

Moscow Physicotechnical Institute
(Submitted November 18, 1976; resubmitted June 17, 1977)
Zh. Eksp. Teor. Fiz. 73, 2008–2029 (December 1977)

It is shown that in the theory of multipomeron exchange with $\alpha_P(0) = (1+\Delta) > \alpha_{cr} > 1$ (in the Froissaron theory), which leads to a Froissart growth of the cross section $\sigma^{tot} \sim \zeta^2$, the problem of s- and t-channel unitarity is connected in radical fashion with the threshold behavior of the pomeron-pole trajectory $\alpha_P(t)$. We investigate the influence of this factor on the t-channel partial amplitude $f(\omega, t)$, where $\omega = j-1$, and on the asymptotic s-channel profile function $F(\zeta, b) = 1-\exp[2i\delta(\zeta, b)]$, where b is the impact parameter. It is shown that, subject to some limitations on the threshold singularity of $\alpha_P(t)$, the amplitude $f(\omega, t)$ does not contradict t-unitarity and, under the same condition at a sufficiently value of the froissaron interaction constant $g_{00} \simeq \Delta^3/a^2$, the function $F(\zeta, b)$ is s-unitarity.

PACS numbers: 11.60.+c

INTRODUCTION

It was noted in a number of papers (see[1] as well as[2-5]) that a pomeron theory with $\alpha_P(0) = (1+\Delta) > 1$, $\Delta \approx 0.1$ agrees well with the experimental data on the growth of the total cross section and of $d\sigma/dt$. By optimal choice of the parameters it is possible to describe simultaneously also a number of properties of particle production processes, such as the distributions in the rapidities and in the multiplicities.[6]

The cited studies dealt in fact with a situation with a "bare" value $\alpha_P(0) > \alpha_{cr} = 1 + \Delta_{cr}$, where $\Delta_{cr} \approx g_{12}^2/\alpha'$, and g_{12} is the vertex of the three-pomeron interaction. In this case it is impossible to carry out the usual program of reggeon field theory with three-pomeron interaction,[7] since all the multipomeron vertices become jumpwise significant at $\Delta > \Delta_{cr}$.[8-10] At ultrahigh energy, when $\xi\Delta > 1$, exchange of "jets" of n pomerons is of importance (Fig. 1a), with $n \sim e^{\xi\Delta}$.[10-12]

In the theory with $\Delta > \Delta_{cr}$ it is convenient to consider, besides the s-channel scattering amplitude $M(\xi, k^2)$ (where $k^2 = -t$), the profile function

$$F(\xi, b) = \frac{2}{i} \int M(\xi, k^2) e^{ikb} \frac{d^2k}{2\pi} = 1 - \exp[2i\delta(\xi, b)],$$

where b is the impact parameter and δ is the scattering phase shift. The function $F(\xi, b)$ has the following characteristic features: it is almost real, close to unity (Fig. 2b) in a wide range of the impact parameter b

$$0 < b < b_0 = a\xi\{1 + O(\xi^{-1} \ln \xi)\}, \tag{1}$$

where a is a certain length (see below). At $b > b_0$ the value of $F(\xi, b)$ decreases exponentially over an interval Δb that does not depend on energy. On this basis, $F(\xi, b)$ was approximated in the literature (see, e. g.,[8]) with the aid of the θ function:

$$F(\xi, b) \to C_0 \theta(b_0 - b). \tag{2}$$

For example, at $C_0 = 1$ this profile corresponds to scattering by a black sphere of radius b_0 with a sharp edge, and leads to a diffraction amplitude $M = M_{b_0}(k)$, where

$$M_b(k) = ib^2 [J_1(kb)/2kb].$$

Actually, the scattering amplitude is connected with the profile function by the relation

$$M(\xi, k^2) = -\frac{i}{2} \int_0^\infty F(\xi, b) J_0(kb) b \, db = \int_0^\infty \left[-\frac{\partial F(\xi, b)}{\partial b} \right] M_b(k) \, db. \tag{3}$$

In the approximation (2) we have $-\partial F/\partial b = \delta(b_0 - b)$, so that the integration in (3) leads to $M_{b_0}(k)$.
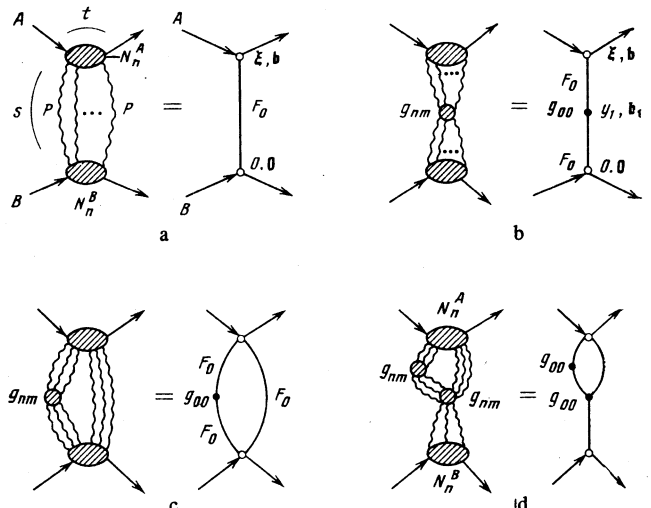

FIG. 1. a) Multipomeron exchange that determines the froissaron, b) enhanced diagrams that include two multipomeron blocks (y_1 and b_1 are the rapidity in the lab system and the impact parameter at the vertex g_{00}); c) and d) different types of froissaron enhanced diagrams consisting of multipomeron blocks.
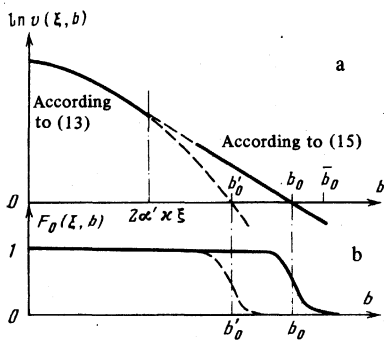
FIG. 2. a) The quantity $\ln v(\xi, b)$ and b) the froissaron profile function $F_0 = 1 - \exp\{-v(\xi, b)\}$ as functions of the impact parameter b; here $b_0' \approx a_0 \xi$, $b_0 = a\xi - \varkappa^{-1} \ln(\eta \xi^{\gamma + 1/2})$. The dashed curves correspond to formula (13).

The profile function in Fig. 2b leads to a Froissart growth[13] of the total cross section $\sigma^{tot} \approx 2\pi a^2 \xi^2$, and at $C_0 = 1$ it leads to diffraction generation with a cross section $\sigma^{diffr} \approx 2\pi a \Delta b \cdot \xi$, so that the corresponding scattering amplitude will be dubbed a *froissaron*.

As noted in the literature,[2,8] the approximation of the froissaron profile by Eq. (2) deviates strongly from the t-channel unitarity condition[14].

$$f(\omega, t) - f^*(\omega^*, t) = 2iA_0(t - \varkappa^2)^{\omega + 3/2} \tilde{f}(\omega, t) f^*(\omega^*, t), \quad (4)$$

which should be satisfied in the interval $(2\varkappa)^2 > t > \varkappa^2 \equiv 4\mu_\pi^2$; A_0 is a certain constant. We use $f(\omega, t)$ to denote the partial t-channel amplitude (continued into the complex plane $j \equiv \omega + 1$), which we shall also call the Green's function of the froissaron. It is known that $f(\omega, t)$ is connected with the s-channel scattering amplitude by the relation

$$f(\omega, t) = \int_0^\infty \text{Im} \, M(\xi, k^2) e^{-\omega \xi} \, d\xi. \quad (5)$$

At $M = M_{b_0}(k)$, $b_0 = a\xi$ this integral yields the well known Schwartz form[2,8]

$$f(\omega, t) \to \int_0^\infty e^{-\omega \xi}(a\xi)^2 J_1(ak\xi) \frac{d\xi}{2ak\xi} = \frac{a^2/2}{(\omega^2 + a^2 k^2)^{3/2}}, \quad (6)$$

which certainly violates the condition (4) near the singular points in the ω plane, i.e., at $\omega \to \pm a\sqrt{t}$. We shall show that this difficulty can be overcome if: a) we forgo the approximation (2) and take into account, when calculating the integral in (3), the logarithmic term (1) as well as of the contribution of the "tail" of the froissaron profile; b) we take into account the threshold singularity of the pomeron trajectory in the form $\bar{\varepsilon}(\varkappa^2 - t)^\gamma$, where $\bar{\varepsilon}$ is a small parameter; c) take into account the contribution of the enhanced diagrams.

When these factors are taken into account, the form (6) of the amplitude $f(\omega, t)$ is preserved only at $|t| \ll \varkappa^2$, whereas at $t \approx \varkappa^2$ the form of $f(\omega, t)$ is entirely different; in particular, near the right-hand singular point $\omega = a\sqrt{t}$ the singular part of $f(\omega, t)$ tends to zero. This makes it possible to satisfy the condition (4) if the regular part of

$f(\omega, t)$ is properly chosen.

The foregoing questions (with the exception of the enhanced diagrams) are considered mainly in Sec. I, which is devoted to the calculation of froissaron profiles $F_0(\xi, b)$ and the Green's function $f_0(\omega, t)$, with account taken of only the non-enhanced diagrams (the zeroth approximation).

The problem of the "enhanced" diagrams[15] of the type, b, c, and d in Fig. 1 is considered in the last section of the article. These diagrams contain chains of "jets" of pomerons, which are connected along the t channel by multipomeron vertices $g_{nm} = g(n, m)$. As $\xi \to \infty$, large $n \sim m \sim e^{\xi\Delta}$ become important, so that the theory with $\alpha_P(0) > \alpha_{cr}$ is substantially different from the case $\alpha_P(0) = \alpha_{cr}$, when only three-pomeron interactions are significant.[7]

To calculate the contribution of the enhanced diagrams b–d of Fig. 1 at $\alpha_P > \alpha_{cr}$ it is convenient to sum first the contributions of the pomerons in each of the "jets," i.e., to form the zeroth-approximation "froissarons" $M_0(y_i, k_i^2)$, and to consider next the diagrams (indicated on the right in Fig. 1) made up of froissaron lines. This is possible, since the contributions of the froissarons can be factored out as $y_i \to \infty$ [8] and their coupling vertices, as shown by Cardy,[8] are equal to $g_{00} = g(0, 0)$ regardless of the number of incoming lines. The combined contribution of these diagrams determines the exact asymptotic scattering amplitude $M(\xi, k^2)$, which also has a profile close to that shown by the solid line in Fig. 2, and which we shall call the *exact froissaron*.

By considering enhanced diagrams of the type b–d of Fig. 1, Cardy[8] reached the conclusion that as $\xi \to \infty$ their contributions cancel each other in each order in g_{00}. It was subsequently shown, however, that this conclusion is utterly incorrect[10-12] and that the sum of all these diagrams fails to violate s-unitarity only at small g_{00} (see also[9]).

We present below a more detailed analysis of this question[12] on the basis of a previously derived[10,11] equation for the combined contribution of all the enhanced diagrams. We investigate the convergence of the method of successive iterations of this equation when the froissaron $F_0(\xi, b)$ (Fig. 1a) is used as the zeroth approximation. It is shown that the method indeed converges and leads to an s-unitarity amplitude at a sufficiently small froissaron interaction constant g_{00} and at $\gamma > 2$, where γ is a parameter that determines the threshold behavior of the pomeron trajectory.

We consider only a moving Pomeranchuk pole with $\alpha_P'(0) > 0$ (in contrast, for example, to the model of Chang and Wu[3,4]), which stems in natural fashion[16] from multiperipheral intermediate states, i.e., diagrams of the ladder type. The simple properties of these states, in combination with the group of reggeon diagram technique[15] and with the rules for "cutting" the diagrams,[17] leads to a connection[6] between the scattering properties and the multiple-production processes. This connection cannot be discerned in the model with immobile pomeron,[3,4] the "anatomy" of which is unknown.

M. S. Dubovikov and K. A. Ter-Martirosyan

In papers by the CERN group,[18-22] the theory with $\alpha_P(0) > \alpha_{cr}$ was investigated with the aid of the formalism of the reggeon field theory (RFT) with account taken of 3 (and $4^{[22]}$)-pomeron interactions on the basis of the lattice approximation. The main object of the analysis was the pomeron propagator, and the principal result was the conclusion that a phase transition takes place when $\alpha_P(0)$ is increased, at the point $\alpha_P(0) = \alpha_{cr}$ at which the formulas of the theory change jumpwise. Our results (see also[9-12]) confirm this conclusion. They also show, however, that at $\alpha_P(0) > \alpha_{cr}$ neglect of the multipomeron interactions is quite inadmissible, since it is precisely these interactions that cause the contribution of the pomeron propagator to the asymptotic amplitude to cancel out exactly. As a result, the problem of the renormalization of a pomeron propagator is hardly of interest at all in the theory with $\alpha_P(0) > \alpha_{cr}$. Questions connected with this fact are considered at the end of the article.

Another important property of the theory with $\Delta > \Delta_{cr}$ is the good agreement with experiment: theory leads to a rapid growth of the total cross sections in the region of attainable energies (in contrast to the other approaches[7,18-23]) and explains in natural fashion the geometric scaling in this energy region, as well as the aggregate of all the data on the production of particles at low transverse momenta.

I. THE GREEN'S FUNCTION OF THE FROISSARON

Assume that the use of only the non-enhanced diagrams of Fig. 1a gives a "good" zeroth approximation of the asymptotic amplitude, and that the enhanced diagrams (Figs. 1b–1d) yield a small correction. The verification of this hypothesis is the gist of the s-unitarity problem, and is the subject of the next section of the article.

The calculation of the contribution of the diagrams of Fig. 1a is easiest in the $(\xi, \mathbf{b})$ representation, in which, according to the Gribov rules,[15]

$$F_0(\xi, b) = \sum_{n=1}^{\infty} \frac{(-1)^{n-1}}{n!} [v(\xi, b)]^n C_n = E(v(\xi, b)), \qquad (7)$$

where $C_n = N_n^A N_n^B / (N_1^A N_1^B)^n$ are dimensionless coefficients $N_n^A (N_1^A = G_A)$ are the vertices for pomeron emission by particles, and $v(\xi, \mathbf{b})$ is the pomeron profile function.

The coefficients C_n are unknown and can only be estimated. To simplify the notation we consider the eikonal model $C_n \equiv 1$, in which

$$F_0(\xi, b) = 1 - e^{-v(\xi, b)}. \qquad (8)$$

As will be seen, the results do not depend on the form of the eikonalization, i.e., on the choice of the function $F_0 = E(v)$; it is necessary only to have $E(v) \ll 1$ at $v \gg 1$ and $E(v) \approx v$ at $v \ll 1$. Another form can be, for example, $C_n = n!$, in which $F_0 = v/(1+v)$, or else from the class of Cardy's models,[8] where $C_n = C(n)$ is an analytic function of n, with $C(n)/\Gamma(n) \to 0$ as $n \to \infty$. For this class we have $E(v) = C(0)$ at $v \gg 1$.

To obtain the profile it is necessary to know the pomeron profile

$$v(\xi, \mathbf{b}) = \int_0^\infty \frac{2}{i} M_P(\xi, k^2) J_0(kb) k \, dk, \qquad (9)$$

where

$$M_P(\xi, k^2) = iG^2 \exp\{[\alpha_P(-k^2) - 1](\xi - i\pi/2) - R^2 k^2\} \qquad (10)$$

is the pomeron amplitude, $\alpha_P(t)$ is the pole trajectory, and R^2 determines the dependence of the residue of the pomeron $G^2 \exp(-R^2 k^2)$ on $t = -k^2$. For simplicity we assume that $G_A = G_B = G$. The amplitude (10) in the j-plane corresponds to the simple pole $[j - \alpha_P(t)]^{-1}$.

1. Threshold singularity and profiles of the pomeron and of the froissaron

We shall show that allowance for the threshold singularity of $\alpha_P(t)$ is of decisive significance for the t- and s-unitarity of the theory. We assume that this is a power-law singularity, so that near $t = \varkappa^2 \equiv 4\mu_\pi^2$ we have

$$\alpha_P(t) = 1 + \Delta + \alpha' t - \bar\varepsilon(\varkappa^2 - t)^\gamma, \qquad (11)$$

where $\bar\varepsilon$ is the small coefficient and γ is some non-integer.

The integral (9) can also be written in the form

$$v(\xi, b) = -i \int_c M_P(\xi, k^2) \mathcal{H}_0^{(1)}(kb) k \, dk$$

$$\approx G^2 \left(\frac{2}{\pi i b}\right)^{1/2} \int_c \exp\{ikb + \xi[\Delta - \alpha' k^2 - \bar\varepsilon(k^2 + \varkappa^2)^\gamma]\} k^{1/2} dk, \qquad (12)$$

so that

$$J_0(x) = \frac{1}{2}[\mathcal{H}_0^{(1)}(x) + \mathcal{H}_0^{(1)}(-x + i\tau)], \quad x > 0, \quad \tau > 0, \quad \tau \to 0.$$

The contour C is indicated on Fig. 3, where the horizontal thick line shows the cut corresponding to the Hankel function $\mathcal{H}_0^{(1)}(kb)$. The right-hand formula in (12) is valid in the region $x = kb \gg 1$ of interest to us, where $\mathcal{H}_0^{(1)}(x) \approx (2/i\pi x)^{1/2} e^{ix}$. The term $\bar\varepsilon(k^2 + \varkappa^2)^\gamma$ in the exponential in (12) should be assumed arbitrarily to be of the same form as at $k^2 \to -\varkappa^2$. Otherwise the integral (5) may diverge. By shifting the integration contour C upward on Fig. 3, we can calculate the integral (12) by the saddle-point method, so long as the saddle-point $k_0 \approx ib/2\alpha' \xi$ lies below the singular point of the integrand, i.e., so long as $\mathrm{Im}\, k_0 < \varkappa$ or at $b < 2\alpha' \varkappa \xi$. If we neglect in the integral of (12) the quantity $\bar\varepsilon(k^2 + \varkappa^2)^\gamma$, then we obtain the known result

$$v(\xi, \mathbf{b}) = (G^2/\alpha'\xi) \exp[\xi\Delta - b^2/4\alpha'\xi], \quad b < 2\alpha'\varkappa\xi, \qquad (13)$$
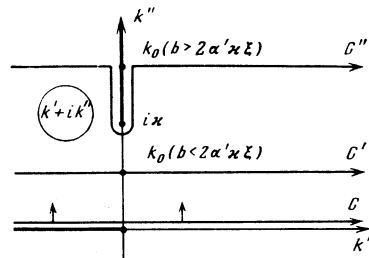

FIG. 3. Integration contour of the integral (12) in the k-plane.

which follows also directly from (9) and (10) at $\bar{\varepsilon} = 0$. Allowance for the singular term at $b < 2\alpha'\varkappa\xi$ in (12) leads to a small shift of the saddle point k_0 and the small corrections in the argument of the exponential ($\Delta \to \Delta - \bar{\varepsilon}(\varkappa^2)^\gamma$, $\alpha' \to \alpha' + \gamma\bar{\varepsilon}(\varkappa^2)^{\gamma-1}$), which are less significant the smaller $\bar{\varepsilon}$.

In the region $b > 2\alpha'\varkappa\xi$, however, where $\text{Im}\, k_0 > \varkappa$, the role of the singular term changes radically. The contour C can be transformed here into C'', which encircles the cut drawn from the branch point $k = i\varkappa$ (Fig. 3) of the function $\alpha_P(-k^2)$ to $k = i\infty$.

If $\gamma > 1$, then the main contribution to the integral (12) is made by the region of small $|k - i\varkappa| \sim 1/\xi$. We can therefore expand $\exp[-\bar{\varepsilon}\xi(k^2 + \varkappa^2)^\gamma]$ in a series and confine ourselves to the first singular term. This yields

$$v(\xi, b) = G^2 \left(\frac{2\varkappa}{\pi b}\right)^{1/2} \int_{C''} [1 - \varepsilon\xi(\varkappa^2 + k^2)^\gamma] e^{\varphi_b(k)} dk,$$

where the function $\varphi_b(k)$ on the vertical cut takes the form

$$\varphi_b(k) = \varkappa(a\xi - b) - r(b - 2\alpha'\varkappa\xi) + \alpha'\xi r^2,$$

while $r = (k - i\varkappa)/i$ is the distance to the singular point $k = i\varkappa$, and the length

$$a = (\Delta + \alpha'\varkappa^2)/\varkappa \tag{14}$$

will play an important role subsequently.

The contour C'' should be bent at the saddle point of the function $\exp[\varphi_b(k)]$, i.e., at $r = r_0 \equiv (\lambda_0/2\alpha') - \varkappa$, where $\lambda_0 = b/\xi$. At this point the function

$$\exp[\varphi_b(k) - \varphi_b(i\varkappa)] \sim \exp\{-\xi(\lambda_0 - 2\alpha'\varkappa)^2/4\alpha'\}$$

has a deep minimum, and therefore integration with respect to the variable $r = -ik - \varkappa$ can be terminated at $r = r_0$ (this result in an exponentially small error). As a result we get

$$v(\xi, b) \approx 2G^2\varepsilon \left(\frac{2\varkappa}{\pi b}\right)^{1/2} e^{\varkappa(a\xi-b)} \int_0^{r_0} e^{-(b-2\alpha'\varkappa\xi)r} (2\varkappa r)^\gamma dr$$

$$\approx B \frac{\xi e^{\varkappa(a\xi-b)}}{\sqrt{b}(b - 2\alpha'\varkappa\xi)^{\gamma+1}} \{1 + O(\xi^{-\gamma})\}; \quad b > 2\alpha'\varkappa\xi, \tag{15}$$

where

$$B = 2G^2\varepsilon\pi^{-1/2}(2\varkappa)^{\gamma+1/2}\Gamma(1+\gamma), \tag{16}$$

$$\varepsilon = \bar{\varepsilon}\sin\pi\gamma > 0. \tag{17}$$

If $\Delta > \alpha'\varkappa^2$ (as is in fact the case) then, as seen from (15) and (14), there exists a wide region $2\alpha'\varkappa\xi < b < a\xi$ in which $v \gg 1$. Therefore the froissaron profile (8) is determined by the profile $v(\xi, b)$ [Eq. (15), but not (13)] in the fall-off region (Fig. 2) and in the "plateau" section.

The next threshold singularities of the trajectory $\alpha_P(t)$ at $t = t_n \equiv (n\varkappa)^2$ result in exponentially small corrections to (15) as $\xi \to \infty$. In fact, the contribution of the n-th threshold comes into play only at $b > 2\alpha'n\varkappa\xi$ and is of the order of $\exp(\xi\Delta + \alpha'n^2\varkappa^2\xi - n\varkappa b)$. At $b > 2\alpha'n\varkappa\xi$ and as $\xi \to \infty$ this quantity is exponentially small in com-

parison with (15).

In the transition region $b \approx 2\alpha'\varkappa\xi$ the arguments of the exponentials in (13) and (15) coincide and it can be shown that the condition (17) $\varepsilon > 0$ ensures positiveness of $v(\xi, b)$ in this region, too.

Thus, the froissaron profile $F_0(\xi, b)$ (8), (13), (15) has a b-dependence of the type shown in Fig. 2, with a plateau in the region $b < b_0$ ($b_0 \approx a\xi$), where $v(\xi, b) \gg 1$, with a fall-off region where $v(\xi, b) \sim 1$, and with a "tail" region at $b > b_0$, where $v(\xi, b) \approx F_0(\xi, b) \ll 1$. The value $b = b_0$ will be obtained by equating the right-hand side of (15) to unity. This yields

$$b_0 = a\xi - [(\gamma + 1/2)/\varkappa]\ln\xi - \varkappa^{-1}\ln\eta, \tag{18}$$

where

$$\eta = B^{-1}a^{1/2}a_-^{\gamma+1}$$

is a certain number, and the length $a_- = a - 2\alpha'\varkappa = (\Delta - \alpha'\varkappa^2)/\varkappa$ is positive at $\Delta > \alpha'\varkappa^2$.

In the fall-off region of the curve of Fig. 2b at $|b - b_0| \ll a\xi$, the profile (15) can be represented in the simple form

$$v(\xi, b) = e^{(b_0-b)\varkappa}, \quad |b - b_0| \ll a\xi. \tag{19}$$

The condition $b_0 > 2\alpha'\varkappa\xi$ for the validity of the formula (15) in the "fall-off" region of the curve of Fig. 2b determines that minimal value of the rapidity $\xi = \xi_0$ at which the profile $F_0(\xi, b)$ is determined by formulas (8) and (15) (or by formula (19)):

$$\xi_0 \geqslant \frac{2\gamma+1}{2a_-\varkappa}\ln\frac{2\gamma+1}{2a_-\varkappa} - \frac{1}{a_-\varkappa}\ln\eta. \tag{19'}$$

At smaller ξ, the froissaron profile $F_0(\xi, b)$ is determined by formulas (8) and (13), which yield much smaller values of b_0 (see Fig. 2):

$$b_0' = 2(\alpha'\Delta)^{1/2}\xi - (\alpha'/\Delta)^{1/2}\ln(\alpha'\xi/G^2).$$

Formulas (8) and (13) determine the $F_0(\xi, b)$ in the (non-realistic) case $\Delta < \alpha'\varkappa^2$, when at $b \approx 2\alpha'\varkappa\xi$ formula (13) already yields $v(\xi, b) \ll 1$. This means that the threshold singularity of $\alpha_P(t)$ manifests itself only in the far region of the "tail," where $F(\xi, b) \ll 1$. It can be shown that at $\Delta < \alpha'\varkappa^2$ allowance for the enhanced diagram leads to violation of s-unitarity. We shall dwell on this case briefly in Appendix I. It is seen (Fig. 2) that allowance for the threshold singularity at $\Delta > \alpha'\varkappa^2$ greatly increases the radius of the froissaron profile, by an amount $b_0 - b_0' = (a - 2\sqrt{\alpha'\Delta})\xi$.

2. Zeroth-approximation froissaron Green's function

Let us find the total contribution of the diagrams of Fig. 1a to the amplitude $M_0(\xi, k^2)$. To this end we substitute $F_0(\xi, b)$ in the form (8) into the right-hand side of (3) and change over to the integration variable $v = v(\xi, b)$. This yields

$$M_0(\xi, k^2) = \int e^{-v}[ibJ_1(kb)/2k]dv. \tag{20}$$

Dependence of b on v is obtained from (19):

$$b = b_0 - \varkappa^{-1} \ln v = a\xi - \varkappa^{-1} \ln(v\eta\xi^{\tau+\frac{1}{2}}). \qquad (21)$$

Substituting expression (20) with allowance for (21) into formula (5), we obtain the zeroth-approximation froissaron Green's function $f_0(\omega, t)$:

$$f_0(\omega, t) = \int_0^{\bar{}} e^{-\tau}\varphi_v(\omega, t)\,dv, \qquad (22)$$

$$\varphi_v(\omega, t) = (2k)^{-1} \int_0^{\infty} e^{-a\xi} b J_1(kb)\,d\xi. \qquad (23)$$

Let us calculate $f_0(\omega, t)$ in the region of interest—near the right-hand singular point in the ω plane (i.e., at $|\omega + iak| \to 0$) and at $t \neq 0$, when an important role in the integral is played by large $\xi \sim |\omega + iak|^{-1}$, and also by large $kb \sim ak\xi$. In this case we can use the asymptotic expansion for the Bessel function

$$J_1(x) = \pi^{-\frac{1}{2}}\{[e^{-ix}/(-2ix)^{\frac{1}{2}}] + [e^{ix}/(2ix)^{\frac{1}{2}}]\},$$

and take the logarithmic term in (21) into account only in the exponentials $\exp(\pm ikb)$. We arrive at the result

$$\varphi_v(\omega, t) = v^{ik/\varkappa}\varphi(\omega, k) + v^{-ik/\varkappa}\varphi(\omega, -k), \qquad (24)$$

$$\varphi(\omega, k) = \frac{a^2\eta^{ik/\varkappa}}{\pi^{\frac{1}{2}}}\Gamma\left(\frac{3}{2} + \left(\gamma + \frac{1}{2}\right)\frac{ik}{\varkappa}\right)(-2iak)^{-\frac{1}{2}}(\omega + iak)^{-\frac{1}{2}-(ik/\varkappa)(\tau+\frac{1}{2})}. \qquad (25)$$

It is seen from (24) and (22) that $f_0(\omega, t)$ has no singularities in the t-plane at $t = 0$. We therefore confine ourselves below to an analysis of this function only in the upper-half plane $k = \sqrt{-t}$.

At $t \equiv -k^2 \neq \varkappa^2$ substitution of (24) and (25) into the integral (22) yields the following expression for the singular part of $f_0(\omega, t)$ near the singular point $\omega = -iak$ in the ω plane:

$$f_0(\omega, t) = \Gamma(1 + ik/\varkappa)\varphi(\omega, k). \qquad (26)$$

This expression is valid at $|\omega + iak| < |ak|$. If we have under this condition also $k \to 0$ (i.e., if $(\omega + iak)$ is of higher order of smallness than ak), then (26) coincides with the Schwartz form (6).

The pole of the Γ function in (25) is due to the divergence of the integral (23) in the $\xi \to 0$ region at $\frac{3}{2} + (ik/\varkappa) \times (\gamma + \frac{1}{2}) = 0$. At small ξ, however, the asymptotic form (20), (21) used above for the amplitude is incorrect. Therefore the lower limit in the integral (23) must be replaced by a certain value ξ_0. This leads to the following change in the (25):

$$\Gamma(\tfrac{3}{2} + (\gamma + \tfrac{1}{2})ik/\varkappa) \to \Gamma(\tfrac{3}{2} + (\gamma + \tfrac{1}{2})ik/\varkappa, (\omega + iak)\xi_0), \qquad (27)$$

where

$$\Gamma(x, y) = \int_y^{\infty} e^{-u}u^{x-1}\,du = \Gamma(x) + \sum_{n=0}^{\infty}\frac{(-1)^{n+1}y^{n+x}}{n!(n+x)} \qquad (27')$$

is the incomplete Γ function, with $x = \frac{3}{2} + (\gamma + \frac{1}{2})ik/\varkappa$, while $y = (\omega + iak)\xi_0$. Near the singular point $\omega \to -iak$ this substitution leads to the appearance of a number of regular terms in (25). The substitution (27) is impor-

tant only at $x \to 0$, $|x| < |y|$.

As $k \to i\varkappa$, the pole of the Γ function in (26) is due to the divergence of the integral (22) in the region of small v. This means that $f_0(\omega, t)$ is determined as $t \to \varkappa^2$ mainly by the "tail" of the profile of $F_0(\xi, \mathbf{b})$. In this region, however, the condition for the applicability of formulas (19) and (21), $|b - b_0| \ll a\xi$, may be violated, and then the result (26) turns out to be incorrect. To calculate $f_0(\omega, t)$ as $t \to \varkappa^2$ it is therefore necessary to use the exact formula (15), and it suffices to confine oneself to the contribution $\bar{M}(\xi, k^2)$ to the integral (3) only in the region $b > b_0 - \varkappa^{-1}\ln\zeta$ ($\zeta \ll 1$ is a certain fixed number). In this region we have $F_0(\xi, \mathbf{b}) \approx v(\xi, \mathbf{b})$ (15), and we arrive at the integral

$$\bar{M}_0(\xi, k^2) = \frac{iB\xi(\varkappa + ik)^{\tau}}{(-2\pi ik)^{\frac{1}{2}}}\exp\{[a - 2\alpha'(\varkappa + ik)]\varkappa\xi\}\int_{x_0}^{\infty} x^{-\tau-1}e^{-x}\,dx,$$

where $x = (\varkappa + ik)(b - 2\alpha'\varkappa\xi)$, and x_0 is the value of x at $b = b_0 - \varkappa^{-1}\ln\zeta$. When $\bar{M}_0(\xi, k^2)$ is substituted in the integral (5) we obtain in the limiting cases the following results:

$$\text{sing}\, f_0(\omega, t) = \frac{-G^2\varepsilon(\varkappa^2 - t)^{\tau}}{(\omega + iak)^2} \quad \text{if} \quad \left|\frac{1 + ik/\varkappa}{\omega + iak}\right| \ll 1; \qquad (28)$$

$$\text{sing}\, f_0(\omega, t) = \frac{\gamma G^2\varepsilon(2\varkappa)^{\tau}(\omega + iak)^{-\frac{1}{2}-(ik/\varkappa)(\tau+\frac{1}{2})}}{(a - 2\alpha'\varkappa)^{\tau+1}(\varkappa + ik)}$$

$$\text{if} \quad \left|\frac{1 + ik/\varkappa}{\omega + iak}\right| \gg 1, \qquad (29)$$

where $\text{sing}\,f_0(\omega, t)$ denotes the principal singular part of $f_0(\omega, t)$ with respect to both arguments $\omega + iak$ and $\varkappa + ik$.

We note that formula (29) follows from (26) in the limit as $|1 + ik/\varkappa| \to 0$, as it should.

It follows from (28) and (29) that at the point $k = i\varkappa$ the singularity of $f_0(\omega, t)$ with respect to the variable ω at $\omega = -iak = a\sqrt{t}$ is "soft" if $\gamma > 2$. It should be noted that the condition $\gamma = \frac{1}{2} + \alpha(\varkappa^2)$ obtained by Gribov and Pomeranchuk[24] in the theory with $\alpha_P(0) = 1$ is not obligatory in the case $\alpha_P(0) > 1$. In fact, in the derivation of this condition from t-unitarity it was assumed in[24] that all the $f(\omega, t)$ terms except the pole term are small as $\omega \to \alpha(t)$ and $t \to \varkappa^2$. This assumption, however, is incorrect if the singularity of the pole term is cancelled out by the sum of the remaining terms of the eikonal series, as is the case when $\alpha_P(0) > 1$. As will be shown below, we reconcile the $\alpha_P(0) > 1$ theory with the t- and s-unitarity conditions it is necessary to have $\gamma > 2$.

Carrying out a transformation inverse to (3) and (5), we obtain

$$F_0(\xi, \mathbf{b}) = \frac{1}{2\pi i}\int_{\dagger} e^{\omega\xi}\,d\omega \int_C f_0(\omega, t)\mathscr{H}_0^{(1)}(kb)k\,dk \qquad (30)$$

and, transforming the integration contour C into C'' (Fig. 3), we can reproduce the froissaron profile (8), (15) in the region of the "tail." All that matters here is the part of $f(\omega, t)$ which is singular in the two arguments $\omega + iak$ and $\varkappa + ik$, whereby (28) accounts for $F_0(\xi, \mathbf{b})$ in the region $b \gg a\xi$, and (29) in the region $a\xi \gg (b - b_0) \gg a$.

The t-unitarity condition (4) near the threshold $t = \varkappa^2$ is best discussed after investigating the enhanced dia-

grams. The point is that besides the principal singularity in the ω plane (i. e., at $\omega = -iak$), the Green's function (22), (23) has at the point $\omega = iak$ a singularity that is obtained when account is taken of the terms $\sim \exp(ikb)$ in the asymptotic formula for the Bessel function. In contrast to (28) and (29), the singularity at the point $\omega = iak$ is not "soft" at $k = i\varkappa$, and takes the form

$$f_0(\omega, t) \approx \text{const} \cdot (\omega - iak)^{-\frac{1}{2} + (ik/\varkappa)(1 + \frac{1}{\varkappa})}, \quad \omega \to iak. \tag{31}$$

For the theory to be compatible with the t-unitary principle it is therefore necessary that the enhanced diagrams alter $f(\omega, t)$ radically (in comparison with $f_0(\omega, t)$) as $\omega \to iak$. On the other hand, for the theory to be compatible with the s-unitarity principle it is desirable that the enhanced diagrams yield small corrections $\Delta f(\omega, t)$ to the function $f_0(\omega, t)$ near the principal singularity $\omega = -iak$ as $k \to i\varkappa$, since the form of $f(\omega, t)$ as $\omega \to -iak$ and $k \to i\varkappa$ governs the behavior of the "tail" of the function of the profile $F(\xi, b)$, which is s-unitary in the zeroth approximation.

We proceed thus to the investigation of the enhanced diagrams.

II. FROISSARON DIAGRAMS AND s-UNITARITY

The investigation of this question is facilitated by the fact that the summation of the pomeron diagrams can be reduced to summation of the froissaron diagrams indicated in the right-hand side of Fig. 1. The point is that each block of the complex diagrams contains in turn the complete (or almost complete) set of pomeron diagrams that make up the froissaron. It is therefore possible to obtain an equation for the amplitude of the exact froissaron.

1. Integral equation for the exact froissaron

As we have shown earlier[10] (see also[11,12]), the sum of all the pomeron diagrams, i. e., the exact froissaron $F(\xi, b)$, is the solution of the equation represented graphically in Figs. 4 and 5. Figure 5 shows that $F(\xi, b)$ takes the form of a series of the type (7) in powers of the profile $V(\xi, b)$—the contribution of the totality of all the irreducible diagrams:

$$F(\xi, b) = \sum_{n=1}^{\infty} \frac{(-1)^{n-1}}{n!} [V(\xi, b)]^n C_n = E(V(\xi, b)), \tag{32}$$

and in the eikonal model we have $F(\xi, b) = 1 - \exp[-V(\xi, b)]$. Diagrams are defined as irreducible (relative to eikonalization) if they cannot be divided in the s-channel (i. e., by a vertical bar) without crossing or cutting even a single pomeron line or a multipomeron vertex.
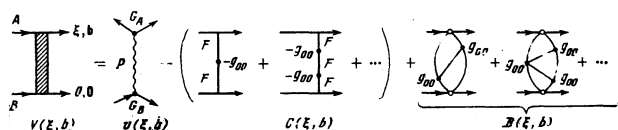
As shown in[10],

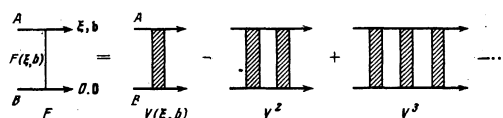FIG. 4. Summary contribution ($V(\xi, b)$ of diagrams that are irreducible with respect to eikonalization.

FIG. 5. Equation for the value $F(\xi, b)$ of the exact froissaron.

$$V(\xi, b) = v(\xi, b) + C(\xi, b) + D(\xi, b) \tag{33}$$

(Fig. 4), where $v(\xi, b)$ is the pomeron profile, and C and D are expressed in terms of the froissaron Green's function in accordance with the Gribov diagram-technique rules.[16]

We recall that the class C (aggregate of chains) includes the irreducible pomeron diagrams that can be divided in the t-channel (i. e., by a horizontal line) without crossing pomeron lines (only multipomeron vertices are crossed). Any diagram of this class contains not less than two links, so that

$$c(\omega, t) = g_{00} z^2(\omega, t)/[1 - g_{00} z(\omega, t)], \tag{34}$$

where g_{00} is the Cardy vertex,[8] and $z(\omega, t)$ and $c(\omega, t)$ are the Green's function of one link and of the sum of all chains, respectively. Obviously, the link includes all the pomeron diagrams with the exception of c (to avoid duplication), i. e., $z(\omega, t) = f(\omega, t) - c(\omega, t)$. Substituting this relation in (34) we arrive at an algebraic equation with respect to $c(\omega, t)$, whose solution is

$$c(\omega, t) = g_{00} f^2(\omega, t)/[1 + g_{00} f(\omega, t)], \tag{35}$$

where $f(\omega, t)$ is the froissaron Green's function with allowance for all the enhanced diagrams.

Relation (35) means that class C can be set in correspondence with the aggregate of diagrams shown in the central part of Fig. 4. The lines correspond to exact froissarons and the vertices to the Cardy constants $(-g_{00})$.

Diagrams of class D (Fig. 4) satisfy the following conditions: 1) It is impossible to divide the diagram in either the s channel or the t channel (by either vertical or a horizontal line) without crossing or cutting a single froissaron line; 2) not less than three lines converge on each vertex; 3) there is not a single fragment of the diagram (with the exception of the froissaron line) that has less than three common vertices in the remaining part.

The property (3) means that if we replace in the diagram of class D the froissaron line by some more complicated fragment, then we obtain a diagram whose contribution has already been taken into account in the initial diagram and needs not be accounted for again. For example, it is not necessary to take into account the contribution of the diagram shown in Fig. 6, since it con-
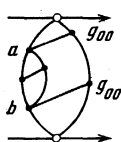

FIG. 6. Example of diagram of class D, which need not be taken into account.

M. S. Dubovikov and K. A. Ter-Martirosyan

tains a fragment connected with the remainder by vertices a and b.

Thus, if we express $C(\xi, \mathbf{b})$ and $D(\xi, \mathbf{b})$ in terms of $F(\xi, \mathbf{b})$ in accordance with the Gribov diagram-technique rules,[15] then (32) and (33) can be regarded as an integral equation for the froissaron amplitude.

The main problem in the investigation of this equation is whether $F(\xi, \mathbf{b})$ (32) can be represented as a series in the small quantity g_{00}, i.e., whether $F_0(\xi, \mathbf{b}) = E(v, \xi, \mathbf{b})$ is a "good" zeroth approximation (at all b). For this purpose it is obviously sufficient to have

$$|V(\xi, \mathbf{b}) - v(\xi, \mathbf{b})| \ll v(\xi, \mathbf{b}), \qquad (36)$$

which means in practice

$$|C(\xi, \mathbf{b})| < v(\xi, \mathbf{b}), \qquad (37)$$

$$|D(\xi, \mathbf{b})| < v(\xi, \mathbf{b}). \qquad (38)$$

Thus, the s-unitarity problem reduces to an investigation of these inequalities, which will be carried out below.

2. Diagrams of class C

At $g_{00} > 0$, besides the diagrams of class C, which have a negative coupling constant $(-g_{00})$, we shall consider an aggregate of diagrams with positive coupling constant g_{00}. The corresponding Green's function $\bar{c}(\omega, t)$ is

$$\bar{c}(\omega, t) = g_{00} f^2(\omega, t) / [1 - g_{00} f(\omega, t)]. \qquad (39)$$

Since $\bar{C}(\xi, \mathbf{b}) \geq |C(\xi, \mathbf{b})|$, it suffices to stipulate satisfaction of the inequality (37) for $\bar{C}(\xi, \mathbf{b})$.[1]

We have investigated in[10] the diagrams C and $\bar{C}$ in approximation (2) for the froissaron profile to which the Green's function (6) corresponds. Substitution of (6) in (39) yields (at $C_0 = 1$)

$$\bar{c}(\omega, t) = \frac{(ga^2/2)(\omega^2 + a^2 k^2)^{-\frac{3}{2}}}{(\omega^2 + a^2 k^2)^{\frac{1}{2}} - g}, \quad g = \frac{a^2 g_{00}}{2}. \qquad (40)$$

As shown in[10], the Green's function (40) corresponds to the profile

$$C(\xi, \mathbf{b}) = \frac{1}{3}\theta(a\xi - b) g^{-\frac{1}{6}}\left(\xi^2 - \frac{b^2}{a^2}\right)^{-\frac{1}{6}}\exp\left[g^{\frac{1}{3}}\left(\xi^2 - \frac{b^2}{a^2}\right)^{\frac{1}{3}}\right], \qquad (41)$$

while the Green's function (35) (with (6) taken into account) corresponds to the profile

$$C(\xi, \mathbf{b}) = -\frac{2\theta(a\xi - b)}{3}\operatorname{Re}\frac{\exp[g^{\frac{1}{3}}\eta_1(\xi^2 - b^2/a^2)^{\frac{1}{3}}]}{\eta_1 g^{\frac{1}{6}}(\xi^2 - b^2/a^2)^{\frac{1}{6}}}, \qquad (42)$$
$$\eta_1 = e^{i\pi/3}.$$

Comparing (41), (42), and (15) we arrive at the conclusion that the condition (37) must inevitably be violated at $(\xi - b/a) \sim \xi^\lambda$, where $\lambda < 1$. A more consistent analysis of $C(\xi, b)$, however, eliminates this difficulty. As shown in Appendix II, formulas (41) and (42) are valid only if the constant g is small enough and $(a\xi - b)/a\xi \gg g^{2/3}/(a\varkappa)^2$, while at larger b it is necessary to use the explicit form (25), (26) of the froissaron Green's function $f_0(\omega, t)$ (with allowance for the substitution (27)). This

question is analyzed briefly in Appendix II for small values of g. The analysis yields the following result: in the region

$$(\ln \xi)/\xi \ll (\xi - b/a)/\xi \ll 1 \qquad (43)$$

we have

$$\ln \bar{C}(\xi, \mathbf{b}) \approx \frac{3a\varkappa}{2\gamma + 1}\left(\xi - \frac{b}{a}\right), \qquad (44)$$

so that when (15) is taken into account we get

$$\frac{\ln \bar{C}(\xi, \mathbf{b})}{\ln v(\xi, \mathbf{b})} \approx \frac{3}{2\gamma + 1} < 1, \qquad (45)$$

i.e., the condition $\bar{C}(\xi, \mathbf{b}) < v(\xi, \mathbf{b})$ is satisfied.

It is interesting to note that relation (45) remains valid if $\exp[\varkappa(b_0 - b)] \gg 1$ (i.e., almost up to the boundary of the plateau region of the froissaron).

We must now consider the condition $|C(\xi, \mathbf{b})| < v(\xi, \mathbf{b})$ in the region $b > b_0$. As already mentioned in Sec. I, the behavior of the profile at $b > b_0$ is determined by the singular part of the Green's function with respect to the two variables $\omega + iak$ and $\varkappa + ik$.

The singular part of $f_0(\omega, t)$ (28), (29) tends to zero if $\gamma > 2$. There is also a regular part of $f(\omega, t)$, which remains finite as $(\omega + iak) \to 0$ and $(\varkappa + ik) \to 0$, and which is determined by the behavior of the froissaron profile at finite ξ. Thus, when $f_0(\omega, t)$ is substituted in (35) (in place of $f(\omega, t)$) the principal singular part of $C(\omega, t)$ is obtained in the form (28), (29) with a small coefficient if g_{00} is small enough. Obviously, if the same coefficient is used, the profile $C(\xi, \mathbf{b})$ remains proportional to $F(\xi, \mathbf{b}) \approx v(\xi, \mathbf{b})$ at $b > b_0$ (i.e., in the region of froissaron "tail," Fig. 2b). Consequently, the inequality (37) is satisfied and the chain does not violate s-unitarity at $b > b_0$.

We point out an important consequence of the foregoing reasoning: the profile of a chain of n links $C_n(\xi, \mathbf{b})$ is determined by a configuration such that almost the entire rapidity is carried by one link, and each of the remaining links carries a finite value of the rapidity.

In fact, were we to substitute in the Green's function

$$c_n(\omega, t) = g_{00}^{n-1}[f(\omega, t)]^n \qquad (46)$$

only the singular part of $f_0(\omega, t)$ (28), (29), then we would arrive at the conclusion that $c_n(\omega, t)$ is of higher order of smallness than $f_0(\omega, t)$, and consequently $C_n(\xi, \mathbf{b}) \ll F_0(\xi, \mathbf{b})$ at $b > b_0$. However, allowance for the regular part of $f(\omega, t)$ in formula (46) alters the situation radically: $C_n(\xi, \mathbf{b}) \sim F_0(\xi, \mathbf{b})$ (at $b \gg b_0$), with a proportionality coefficient that depends on the regular part of $f_0(\omega, t)$, which in turn is determined by the behavior of $F_0(\xi, \mathbf{b})$ at finite ξ, when the froissaron profile no longer has the form of Fig. 2b.

3. Diagrams of class D

Let us consider some properties of diagrams of class D. Assume that some diagram of this class has vertices
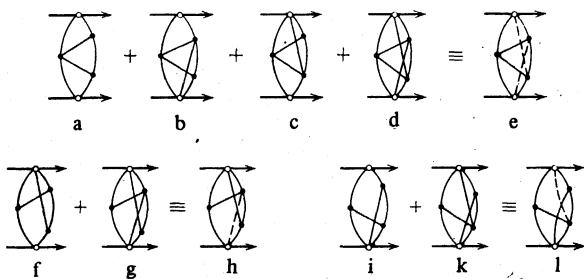
FIG. 7. Diagrams containing cancellation lines.

FIG. 9. Inequality of contributions of diagrams of class D at $b \approx b_0$.

that are not interconnected by a froissaron line. When any pair of such vertices is connected by a froissaron line, we obtain again a diagram of class D (Figs. 7a and 7b).[2] We shall refer to the resultant diagram as supplementary with respect to the initial one, and call the operation itself supplementation. Obviously, the signs of the supplementary and initial diagrams are opposite, and their contributions cancel out completely if the θ-function approximation is used for the froissaron profile (the Cardy cancellation[8]). In a real case the cancellation takes place at $b < a\xi$. On this basis, the summation of the initial and supplementary diagrams will be called a cancellation operation with respect to those vertices between which a froissaron line is drawn in the supplementation operation. We represent the cancellation operation graphically by a dashed line (which we call the cancellation line) joining the corresponding vertices (Fig. 7f, g, h).

We shall call a diagram of class D non-simplifiable if it is impossible to discard from it even a single froissaron line and obtain thereby a diagram that still belongs to class D. Obviously, all the diagrams of class D can be obtained from non-simplifiable ones by performing in them, in succession, the supplementation operation. Therefore any diagram of class D can be represented as an aggregate of non-simplifiable diagrams in which cancellation lines are drawn (Fig. 7). It must only be recognized that the same supplementary diagram can be obtained from different initial diagrams. It can be verified nevertheless that in all the non-simplifiable diagrams of order higher than the second it is possible to draw cancellation lines in such a way that the supplementary diagrams are not taken into account again (see, e.g., Fig. 7). Therefore a Cardy cancellation takes place at $b < b_0$ (the plateau region of the froissaron) and the condition (38) is satisfied.

We investigate now the condition (38) at $b > b_0$ (the region of the froissaron "tail") and at $b \approx b_0$.

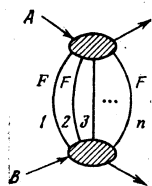In the region $b > b_0$, the profile of any diagram is de-

termined by the singularities of the Green's function in the k plane. The position of the singularities of the D diagram is determined by the equality $k = im\varkappa$, where m is the number of froissarons that can be cut by a horizontal line. Obviously, in this diagram m can assume several values, and some values of m can be repeated when different cuts are drawn. If $\gamma > 2$, then the asymptotic form of the profile of a given diagram at $(b - b_0) \gg a$ is determined by the sum of the contributions of such configurations that the cut froissaron take on practically the entire rapidity ξ, while the remaining lines take on a finite value of the rapidity.

Thus, at $b > b_0$ the sum of all the D diagrams can be represented by the diagram shown in Fig. 8, where the shaded vertices constitute diagrams with finite values of the rapidity. We arrive at the conclusion that condition (38) reduces to the problem of the convergence of the froissaron diagrams at finite rapidity. It is natural to assume that the answer to this question is in the affirmative and condition (38) is then satisfied.

Finally, let us dwell briefly on the region $b \approx b_0$. It can be shown that owing to the presence of a logarithmic term in formula (18) at

$$(b_0 - b) < [(2\gamma + 1)/2\varkappa] \ln \xi$$

the principal contribution to $D(\xi, \mathbf{b})$ is made by the simplest diagrams D_0 (Fig. 9), which contain a minimum number of links along the t channel. The upper bound of the sum of these diagrams (in absolute value) can be represented by the diagram $\tilde{D}_0$ (Fig. 9). At

$$b \approx b_0 - [(2\gamma + 1)/2\varkappa] \ln \xi$$

the contribution of $\tilde{D}_0$ is of the order of ξ_0^3, where the pomeron profile is $\sim \xi^{\gamma + 1/2}$. Thus, at $\gamma > 5/2$ the condition (38) is satisfied. With further decrease of b, the inequality (38) becomes stronger.

4. Discussion of the t-unitarity problem.

The reggeon diagram technique formalism[15] is intended to calculate the asymptotic form of the scattering amplitude in the s channel at $k^2 = -t > 0$ (or of the asymptotic profile function in the s channel), which is determined by the singular part of the t-channel partial amplitude. This part of the amplitude need not, generally speaking, satisfy the t-unitarity condition (4), but it must be such that the condition (4) can be satisfied given a suitable regular part of $f(\omega, t)$. It is very important here to continue $f(\omega, t)$ accurately into the region $t > \varkappa^2$, where the condition (4) is valid. Thus, for example, failure to understand that the Schwartz formula (6) is valid only in the region $|ak| \ll 1$ has led to the incorrect conclu-

FIG. 8. Summary contributions of all D diagrams at $b > b_0$.

1059   Sov. Phys. JETP 46(6), Dec. 1977

M. S. Dubovikov and K. A. Ter-Martirosyan   1059

sion[2,8] that the Froissart growth of the cross section contradicts t-unitarity. Actually, as we have shown, the behavior of $f(\omega, t)$ as $t \to \varkappa^2$ is determined by the "tail" part of the froissaron profile. As a result, the condition (4) can be satisfied near the singularity $\omega = iak \to -a\varkappa$ where the zeroth-approximation Green's function is of the form (31).

We substitute in the eikonal series (32) expressions (33) and (35) and change over to the $(\omega, \mathbf{k})$ representation. The only term in the right-hand side, which has a threshold singularity at $k = i\varkappa$, $\omega \to iak$, is obviously $c(\omega, t)$, i.e.,

$$f(\omega, t) = c(\omega, t) + \mathscr{F}(\omega, t), \qquad (47)$$

where the function $\mathscr{F}(\omega, t)$ has no threshold singularity at $t = \varkappa^2$, $\omega - iak$. From (35) and (47) we obtain

$$f^{-1}(\omega, t) = \mathscr{F}^{-1}(\omega, t) + g_{00}(t); \quad \omega \to iak. \qquad (48)$$

This expression satisfies the condition (4) if the part of the vertex $g_{00}(c)$ with the threshold singularity is equal to $A_0(k^2 + \varkappa^2)^{\omega + 3/2}$.

No such reasoning can be used near $\omega = -iak \to -a\varkappa$, for if we go to the $(\omega, \mathbf{k})$ representation in the right-hand side of (32), then not only $c(\omega, t)$ but also the pomeron term has a threshold singularity at $t = \varkappa^2$.

Near the singularity $\omega = -iak \to -a\varkappa$, the t-unitarity condition can be satisfied by taking into account the background part of $f(\omega, t)$, which makes no contribution to the integral (30). For example, if the background part of $f(\omega, t)$ is of the form

$$C_1 + C_2(\varkappa^2 + k^2)^{\frac{1}{2} + \alpha(\varkappa^2)} + C_3(\varkappa^2 + k^2)^{2 + m}/(\omega + iak)^2$$

at $|(1 + ik/\varkappa)/(\omega + iak)| \ll 1$, and at the same time $\gamma = \frac{5}{2} + m + \alpha(\varkappa^2)$ in the singular part (28) of $f(\omega, t)$, then the condition (4) can be satisfied in the lowest orders in $\varkappa^2 + k^2$. This condition can always be satisfied in the higher orders, since we are free to choose singular terms of $f(\omega, t)$ of higher order of smallness and due to the subsequent singular corrections to the pomeron trajectory.

CONCLUSION

As already noted, interest in the theory with $\alpha_P(0) > \alpha_{cr} > 1$ is due primarily to the possibility of successfully describing with its aid all the presently known experimental data for the region of high energy and small $p_\perp$. We deem it therefore very important to ascertain whether the theory satisfies such fundamental requirements as s- and t-unitarity as $\xi \to \infty$. Our principal result is the conclusion that an affirmative answer to this question can indeed be obtained if the threshold behavior in the t-channel of the pomeron trajectory is correctly taken into account.

Yet one can raise the question of what form the theory of the pomeron itself assumes in the froissaron-exchange scheme developed here. Consider the renormalization of the bare pomeron propagator $S(\omega, k)$, defined by the usual relation
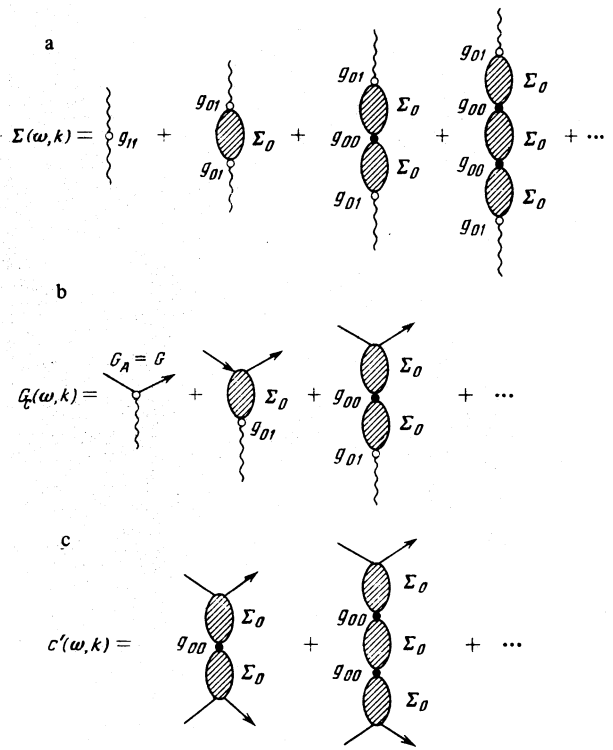

FIG. 10. Diagrams for the self-energy part of the pomeron (a), for the vertex of the coupling of the pomeron with the particles (b), and for the chain $c'(\omega, k)$ (c).

$$S^{-1}(\omega, k) = \omega - \omega_0(k) - \Sigma(\omega, k), \qquad (49)$$

where

$$\omega_0 = \alpha(-k^2) - 1, \quad \alpha(-k^2) = \alpha_0(-k^2) - g_{11}, \quad \omega_0(0) = \Delta,$$

where the self-energy part $\Sigma(\omega, k)$ is determined in the theory with $\alpha(0) > \alpha_{cr}$ by the contribution of chains of the type of Fig. 10a, as well as by the contribution of the vertex for the transition of the pomeron into a pomeron $g_{11} = [g(n, m)]_{n=m=1}$, in the form

$$\Sigma(\omega, k) = g_{01}^2 \Sigma_0(\omega, k)/[1 - g_{00}\Sigma_0(\omega, k)] + g_{11}. \qquad (50)$$

We use next the factorization relation

$$g_{00}g_{11} = g_{01}^2, \qquad (51)$$

and assume that $g_{01} = g_{00}G$, $g_{11} = g_{00}G^2$, where $G_A = G_B = G$. These greatly simplify the calculations without changing the fundamental results. Then formula (50) can be rewritten in the form

$$\Sigma(\omega, k) = g_{11}/[1 - g_{00}\Sigma_0(\omega, k)]. \qquad (52)$$

Obviously, $\Sigma_0(\omega, k)$ is connected with the link $z(\omega, k)$ of the chain C (34) by the relation

$$g_{00}\Sigma_0(\omega, k) = g_{00}z(\omega, k) - g_{11}/[\omega - \omega_0(k)], \qquad (53)$$

since the pole term enters in the link $z(\omega, k)$ but must not enter, by definition, in the link $\Sigma_0(\omega, k)$. Substituting (52) and (53) in (49), we arrive at the expression

$$S(\omega, k) = \frac{g_{11} + (\omega - \omega_0)(1 - g_{00}z)}{(1 - g_{00}z)(\omega - \omega_0)^2}. \qquad (54)$$

We see that the renormalization has led to an appreciable deformation of the pomeron propagator.

To calculate the contribution of the renormalized pomeron to the scattering amplitude it is necessary to take into account also the renormalization of the vertex for the emission of a pomeron by particles. As seen from Fig. 10b, the renormalized vertex $G_c(\omega, k)$ is of the form

$$G_c(\omega, k) = \frac{G}{g_{11}} \Sigma(\omega, k) = \frac{G(\omega - \omega_0)}{(1 - g_{00}z)(\omega - \omega_0) + g_{11}}, \qquad (55)$$

Therefore the contribution of the renormalized pomeron to the t-channel partial waves is

$$f_P^{(0)}(\omega, k) = G_c^2(\omega, k) S(\omega, k) = \frac{G^2/(1 - g_{00}z)}{(1 - g_{00}z)(\omega - \omega_0) + g_{11}}. \qquad (56)$$

Thus, the renormalization of the contribution of the pomeron leads to a shift of the pole to the left, by an amount

$$\Delta\omega_0(k) = -g_{11}/(1 - g_{00}z_0), \quad z_0 = z(\omega_0(k), k).$$

It must be recognized, however, that the complete set of the irreducible (with respect to eikonalization) diagrams contains also the chains C', whose links contain no single-pomeron exchanges at all (Fig. 10c). The sum $c'(\omega, k)$ of the contribution of these diagrams also has a pomeron pole:

$$c'(\omega, k) = \frac{g_{00}\Sigma_0^2(\omega, k)}{1 - g_{00}\Sigma_0(\omega, k)} = \frac{G^2}{g_{11}} \frac{[g_{11} - (\omega - \omega_0)g_{00}z]^2}{[(1 - g_{00}z)(\omega - \omega_0) + g_{11}](\omega - \omega_0)}. \qquad (57)$$

In the sum with $f_P^{(0)} = G_c^2 S$ this reconstructs exactly the pomeron contribution $G^2/[\omega - \omega_0(k)]$ in the sum with the contribution $c(\omega, k)$ of the previously investigated chain (34):

$$f_P(\omega, k) = f_P^{(0)} + c' = \frac{G^2}{\omega - \omega_0} + c(\omega, k), \qquad (58)$$

where $c(\omega, k) = g_{00}z^2(\omega, k)/[1 - g_{00}z(\omega, k)]$ is the quantity (34) which has no pomeron pole; its singular point in the ω plane are located to the left of $\omega = \omega_0(k)$ (see Sec. II).

This result shows that the answer does not depend on the order of the summation of the diagrams (therefore, in particular, it remains valid also when relation (51) between the pomeron vertices is violated). It also eliminates the confusion concerning this question in the literature,[19,21] namely, in the contribution $f_P^{(0)}(\omega, k)$ (56) of the pomeron the pole is shifted to the left, while in the complete set of all the irreducible (with respect to eikonalization) diagrams it turns out to coincide with the bare pomeron.

It was impossible to present in a single article a complete analysis of all the questions touched upon in the text, especially the s-unitarity problem. We have therefore relegated an appreciable part of the calculations to the Appendices. It was impossible, for example, to present even a brief analysis of the conditions $|C(\xi, b)| < v(\xi, b)$ and $|D(\xi, b)| < v(\xi, b)$ in the important region $b \approx b_0$ of the decrease of the profile on Fig. 2. Therefore

only the final results were presented. In addition, we did not touch upon the problem of the exact determination of the right-hand side of the inequality $g_{00} < A_0\Delta^3/\alpha'$, which imposes a restriction on the Cardy vertex on the basis of the s-unitarity requirement.[10] This question will be dealt with in a separate article.

APPENDIX I

FROISSARONS AT $\Delta < \alpha' \varkappa^2$

In this case the condition $v(\xi, b_0) = 1$, which determines the boundary of the froissaron plateau, is satisfied at $b_0 < 2\alpha' \varkappa \xi$, and the froissaron profile in its principal part is determined by substituting (13) in (8) (Fig. 2b, dashed line).

We present without proof an expression for the principal singular term of the Green's function in the froissaron in the case $\Delta < \alpha' \varkappa^2$ at $k^2 < 0$:

$$f_0(\omega, t) = \Gamma(1 + ik\sqrt{\alpha'/\Delta})\varphi(\omega, t), \quad 0 < \text{Im } k < \sqrt{\Delta/\alpha'}; \qquad (I.1)$$

here

$$\varphi(\omega, t) = 2\alpha'\Delta\pi^{-1/2}\Gamma(^3/_2 + ik\sqrt{\alpha'/\Delta}) \cdot$$
$$(\alpha'/G^2)^{ik\sqrt{\alpha'/\Delta}}(-4ik\sqrt{\alpha'\Delta})^{-1/2}(\omega + 2ik\sqrt{\alpha'\Delta})^{-1/2 - ik\sqrt{\alpha'/\Delta}}. \qquad (I.2)$$

Thus, in the region $0 < \text{Im } k < \sqrt{\Delta/\alpha'}$ summation of the eikonal series yields in the ω plane a singularity that has a trajectory $a_0\sqrt{t}$ (where $a_0 = 2\sqrt{\alpha'/\Delta}$), even though the terms of the series have singularities at $\omega = \omega_n = n\Delta + \alpha' t/n$. In the region

$$\sqrt{\Delta/\alpha'} < \text{Im } k < 2\sqrt{\Delta/\alpha'}$$

the single-pole term of the eikonal series is separated, and the sum of the remaining terms has a singularity on the trajectory $\omega = a_0\sqrt{t}$, so that

$$f_0(\omega, t) = \Gamma(1 + ik\sqrt{\alpha'/\Delta})\varphi(\omega, t)$$
$$+ G^2/(\omega - \Delta + \alpha' k^2) \quad \text{at} \quad \sqrt{\Delta/\alpha'} < \text{Im } k < 2\sqrt{\Delta/\alpha'} \qquad (I.3)$$

(if $\frac{3}{2} + ik\sqrt{\alpha'/\Delta} \approx 0$, then it is necessary to carry out in the expression (I.2) for $\varphi(\omega, t)$ (I.2) a replacement of the Γ function, similar to (27)). In the region

$$2\sqrt{\Delta/\alpha'} < \text{Im } k < 3\sqrt{\Delta/\alpha'}$$

the single-pomeron and two-pomeron terms are separated from the eikonal series, and so on.

The separation of the one-pomeron term at $t > \Delta/\alpha'$ was indicated in Cardy's paper,[8] where an erroneous hypothesis was advanced, that the point $t = \Delta/\alpha'$ is singular for $f_0(\omega, t)$. It can be shown by an accurate analysis that the behavior of $f_0(\omega, t)$ near $t = \Delta/\alpha'$ is determined by the expression

$$f_0(\omega, t) \approx \frac{G^2(\omega + i2k\sqrt{\Delta\alpha'})^{-1/2 - ik\sqrt{\alpha'/\Delta}}}{(\omega + 2ik\sqrt{\Delta\alpha'})^{1/2} + (\sqrt{\Delta} + ik\sqrt{\alpha'})}. \qquad (I.4)$$

We can therefore conclude that the one-pomeron singularity (pole) goes over at $t = \Delta/\alpha'$ from the second sheet of the ω plane to the first.

In addition, it has not been noted in[8] that with increasing t the singularity of $f_0(\omega, t)$ becomes "softer" at the point $\omega = a_0\sqrt{t}$ (I.2).

M. S. Dubovikov and K. A. Ter-Martirosyan   1061

It can be shown that in the case $\Delta < \alpha' \varkappa^2$ allowance for the enhanced diagrams leads to violation of s-unitarity.

APPENDIX II

SUPPLEMENT TO THE ANALYSIS OF THE DIAGRAMS OF CLASS C

We shall show first that even at sufficiently small Cardy constant formula (41) is valid only at $(a\xi - b)/a\xi \gg g^{2/3}/(a\varkappa)^2$. We calculate $C(\xi, b)$ accurate to a pre-exponential factor. We can then write down a formula similar to (12):

$$\bar{C}(\xi, b) \sim \int_{-\infty}^{\infty} e^{ikb + \omega_0(k)\xi} \, dk, \tag{II.1}$$

where $\omega_0(k)$ is the position of the right-hand pole of $\bar{c}(\omega, k)$. From (40) we obtain

$$\omega_0(k) = (g^{2/3} - a^2 k^2)^{1/2}. \tag{II.2}$$

The integral (II.1) is calculated by the saddle-point method. The position of the saddle point is found to be

$$k_0 = ibg^{1/3}/[a(a^2\xi^2 - b^2)^{1/2}], \tag{II.3}$$

and we arrive at the argument of the exponential in (41).

Formulas (6) and (40) are valid at $|k| \ll \varkappa$, $(\omega + iak)^{-1} > \xi_0$ (19'). It is clear that $|\omega + iak| \sim \bar{N}/\xi$, where $\bar{N}$ is the average multiplicity of the links in the chain (40). By the standard method we can obtain $\bar{N} = \frac{1}{3} g^{1/3} \xi$. Therefore formulas (II.2), (II.3), (40)–(42) are valid at $g^{1/3} < 1/\xi_0$, $(a\xi - b)/a\xi \gg g^{2/3}/(a\varkappa)^2$, and to calculate $\bar{c}(\xi, b)$ at larger b it is necessary to substitute the Green's function (25), (26) in formula (39).

In particular, it turns out that at $0 < (a\xi - b)/a\xi \lesssim g^{2/3}/(a\varkappa)^2$ the behavior of $\bar{C}(\xi, b)$ is determined by the values of $\bar{c}(\omega, k)$ in the region of small x, where

$$x(k) = \frac{1}{2} + i(\gamma + \frac{1}{2}) k/\varkappa. \tag{II.4}$$

In the region $|x| \ll 1$ the argument of the Γ function in (25) is small, so that it is necessary to make the substitution (27). When account is taken of this substitution and of the expansion (27'), we arrive at the following expression for the froissaron Green's function (25), (26), in the region (II.4) of small x:

$$f(\omega, t) = a^2\lambda(\omega + iak)^{-x} x^{-1}\{1 - [(\omega + iak)\xi_0]^x\}; \tag{II.5}$$

here

$$\lambda = \pi^{-1/2} \eta^{-3/(2\gamma+1)} \left(\frac{2\gamma+1}{6a\varkappa}\right)^{x} \Gamma\left(\frac{2\gamma-2}{2\gamma+1}\right). \tag{II.6}$$

When (II.5) is substituted in (39), the function $\bar{c}(\omega, k)$ acquires a pole at the point $\omega = \omega_0(k)$, where

$$\omega_0(k) = -iak + [G(x)]^{-1/x}, \tag{II.7}$$

$$G(x) = \bar{x}(\lambda g)^{-1} + \xi_0^x. \tag{II.8}$$

We substitute the value $\omega_0(k)$ (II.7) in formula (II.1) and calculate the integral in (II.1) by the saddle-point method. The position of the saddle point k_0 is determined by the following condition:

$$\frac{a\xi - b}{a\xi} = \frac{G(x_0)\ln G(x_0) - x_0 G'(x_0)}{x_0^2 [G(x_0)]^{1+1/x_0}}, \tag{II.9}$$

where $x_0 = x(k_0)$. It can be verified by a simple analysis that this condition is satisfied at $x_0 < 0$, $|x_0| \ll 1$, which corresponds, according to (II.4), to the position of the saddle point $k_0 \approx i3\varkappa(2\gamma + 1)$. In addition, it can be concluded from (2.9) that

$$[G(x_0)]^{-1/x_0} \ll \frac{a\xi - b}{a\xi} \frac{3a\varkappa}{2\gamma+1}. \tag{II.10}$$

If we substitute in the integral (II.1) the value ω_0 (II.7) at the saddle point $k_0 \approx i3\varkappa/(2\gamma + 1)$, and also take the inequality (II.10) into account, then we arrive at formula (44).

We note that the presented analysis is valid at sufficiently small g. The point is that in expression (II.5) we have neglected a certain constant f^0 that results from the contribution of the region of finite values of ξ to $f(\omega, t)$. In order for this term to be inessential when $f(\omega, t)$ is substituted in formula (39), it is necessary to satisfy the condition $gf^0 < 1$.

---

[1] We note that when the conditions (37) and (38) are satisfied it is possible to substitute in formulas (35) and (39), in the zeroth approximation, the Green's function $f_0(\omega, t)$ obtained with only non-enhanced diagrams taken into account.

[2] We recall that it is not permissible to join only vertices that are connected with particles A and B, for this joining results in a reducible diagram.

---

[1] A. Capella and J. Kaplan, Phys. Lett. B **52**, 448 (1974); A. Capella, J. Tran Thanh Van, and J. Kaplan, LPTHE 75/12, 1975.

[2] J. B. Bronzan and C. E. Jones, Phys. Rev. **160**, 1494 (1967).

[3] H. Cheng and T. T. Wu, Phys. Rev. Lett. **24**, 1465 (1970); Phys. Rev. D **1**, 537 (1971).

[4] S. J. Chang and T. M. Yan, Phys. Rev. Lett. **25**, 1586 (1970); Phys. Rev. D **4**, 537 (1971); S. Auerbach, R. Aviv, R. Blankenbeckler, and R. Sugar, Phys. Rev. Lett. **28**, 522 (1972); Phys. Rev. D **6**, 2216 (1972); S. J. Chang, J. K. Wolker, and T. T. Wu, Phys. Lett. B **44**, 97 (1974); Phys. Lett. B **44**, 283 (1974).

[5] L. D. Solov'ev, Pis'ma Zh. Eksp. Teor. Fiz. **18**, 455 (1973); **19**, 185 (1974) [JETP Lett. **18**, 268 (1973); **19**, 116 (1974)]; L. D. Solov'ev and A. V. Shchelkachev, Fiz. Elem. Chastits At. Yadra JINR **6**, 3 (1975) [Sov. J. Part. Nucl. **6**, 1 (1975)].

[6] A. M. Lapidus, V. I. Lisin, K. A. Ter-Martirosyan, and P. E. Volkovitsky, ITEP-115, 1976; Yad. Fiz. **24**, 1237 (1976) [Sov. J. Nucl. Phys. **24**, 648 (1976)]; K. A. Ter-Martirosyan, Phys. Lett. B **44**, 377 (1973); K. A. Ter-Martirosyan, and Yu. M. Shabel'skiĭ, Yad. Fiz. **25**, 403, 670 (1977) [Sov. J. Nucl. Phys. **25**, 217 , 356 (1977)].

[7] A. A. Migdal, A. M. Polyakov, and K. A. Ter-Martirosyan, Preprint ITEP-102, 1973; Zh. Eksp. Teor. Fiz. **67**, 848 (1974) [Sov. Phys. JETP **40**, 999 (1974)].

[8] J. D. Cardy, Nucl. Phys. B **75**, 413 (1974).

[9] B. Z. Kopeliovich and L. I. Lapidus, Zh. Eksp. Teor. Fiz. **71**, 61 (1976) [Sov. Phys. JETP **44**, 31 (1976)]; B. Z. Kopeliovich, Preprint Leningr. Inst. Nucl. Phys., 1977.

[10] M. S. Dubovik and K. A. Ter-Martirosyan, Preprint ITEP-37, 1976; Proc. Coral Gables Conf., Ordis Sciential 11, 313 (1976).

[11] M. S. Dubovikov, B. Z. Kopeliovich, L. I. Lapidus, and K. A. Ter-Martirosyan, Preprint D2-9789 JINR, 1976; Nucl. Phys. B **123**, 147 (1977).

1062   Sov. Phys. JETP 46(6), Dec. 1977

M. S. Dubovikov and K. A. Ter-Martirosyan   1062

[12]M. S. Dubikov and K. A. Ter-Martirosyan, Preprint TH-2262-CERN, 1976; Nucl. Phys. B 124, 163 (1977).

[13]M. Froissart, Phys. Rev. 123, 1053 (1961).

[14]V. N. Gribov, Zh. Eksp. Teor. Fiz. 41, 1962 (1961) [Sov. Phys. JETP 14, 1395 (1962)].

[15]V. N. Gribov, Zh. Eksp. Teor. Fiz. 53, 654 (1967) [Sov. Phys. JETP 26, 414 (1968)]; V. N. Gribov and A. A. Migdal, Zh. Eksp. Teor. Fiz. 55, 1498 (1968) [Sov. Phys. JETP 28, 784 (1969)]; Yad. Fiz. 8, 1002, 1213 (1968) [Sov. J. Nucl. Phys. 8, 583, 703 (1969)].

[16]M. S. Dubovikov, Yad. Fiz. 23, 456 (1976) [Sov. J. Nucl. Phys. 23, 239 (1976)].

[17]V. A. Abramovskiĭ, V. N. Gribov, and O. V. Kancheli, Yad. Fiz. 18, 595 (1973) [Sov. J. Nucl. Phys. 18, 308 (1974)]; E. S. Lahman and G. A. Winbow, Nucl. Phys. B 89, 397 (1975); M. Ciafaloni and G. Marchesini, Preprint TH-2107-CERN, 1975.

[18]D. Amati, M. Ciafaloni, M. Le Bellac, and G. Marchesini, Nucl. Phys. B 112, 107 (1976); Nucl. Phys. B 114, 483 (1976).

[19]H. D. I. Abarbenel, J. B. Bronzan, R. L. Sugar, and A. Schwimmer, Preprint SLAC-PUB 1619, 1976.

[20]M. Moshe, Univ. of Calif. Preprint UCSC 77/118, 1977.

[21]A. R. White, Preprint TH-2259, CERN, 1976.

[22]J. B. Bronzan and R. L. Sugar, Preprint UCSB TH-77-1.

[23]M. S. Dubovikov, Yad. Fiz. 25, 865 (1977 [Sov. J. Nucl. Phys. 25, 461 (1977)].

[24]V. N. Gribov and I. Ya. Pomeranchuk, Zh. Eksp. Teor. Fiz. 43, 308 (1962) [Sov. Phys. JETP 16, 220 (1963)].

Translated by J. G. Adashko

On the existence of a quadrupole moment in muonium

V. G. Baryshevskiĭ and S. A. Kuten'

Belorussian State University
(Submitted April 22, 1977)
Zh. Eksp. Teor. Fiz. 73, 2030–2035 (December 1977)

It is shown that even in its ground-state, muonium (hydrogen, mu-nucleonic atom) has a quadrupole moment which is comparable in magnitude to nuclear quadrupole moments. This leads to a pronounced effect of inhomogeneous intracrystalline fields on the spin precession and relaxation of μ^+ mesons and may serve as a basis for carrying out experiments with muonium (mu-nucleonic atoms) which are analogous to quadrupole resonance and relaxation.

PACS numbers: 36.10.Dr

It is well known that the principal quantum characteristic of muonium is its magnetic moment. It is specifically the existence of this magnetic moment that gave rise to the meson method for studying properties of matter, a distinctive analogue of NMR and EPR, and to its intensive development in recent times (cf., the review article[11]). It will be shown below that muonium in its ground state has yet another quantum characteristic—a quadrupole moment. The existence of a quadrupole moment in muonium opens up new possibilities in the meson method associated with the investigation of quadrupole splitting of muonium levels and of the mechanism of its quadrupole relaxation in matter. In this sense the meson method becomes similar to nuclear quadrupole resonance and can be utilized to study not only magnetic but also inhomogeneous intracrystalline electric fields.

At first sight the assertion made above contradicts the well-known circumstance that as a result of spherical symmetry of the Coulomb interaction the ground 1S-state of muonium (of a hydrogen atom, and of other hydrogen-like systems) is described by a spherically symmetric wave function. As a consequence of this the aforementioned systems should not have any electric multipole moments. However, it is necessary to note that a violation of central symmetry, although insignificant at first sight, arises as a result of the hyperfine interaction between the spins of the electron and of the μ^+ meson in muonium (μ^- meson and the nucleus in a mesic atom, etc.). As a result of this the ground state does not have spherical symmetry and the appearance becomes possible of a quadrupole moment[2] comparable, as it turns out, in order of magnitude with nuclear quadrupole moments. Indeed, the energy of the hyperfine interaction, for example, in the system μ^+e^- can be written in the form[3]

$$V(\mathbf{r}, \mathbf{s}, \mathbf{i}) = V_1(r)\sigma_1\sigma_2 + V_2(r)\{3(\sigma_1\mathbf{n})(\sigma_2\mathbf{n}) - \sigma_1\sigma_2\}', \quad (1)$$

where

$$V_1(r) = -\tfrac{8}{3}\pi\mu_1\mu_2\delta(\mathbf{r}), \quad V_2(r) = -\mu_1\mu_2/r^3, \quad \mathbf{n} = \mathbf{r}/r,$$

$\boldsymbol{\sigma}$ are the Pauli matrices, $\mathbf{s} = \tfrac{1}{2}\sigma_1$, $\mathbf{i} = \tfrac{1}{2}\sigma_2$, μ_1 is the magnetic moment of e^-, μ_2 is the magnetic moment of μ^+.

In the usual analysis of the hyperfine splitting of levels of atoms which are in the ground 1S state the second term in (1) is not taken into account since on averaging over a spherically symmetric state it is equal to zero.[3] However, the interaction proportional to V_2 can admix to the triplet state of muonium, for example, the $^3D_1$ state. As a result of this, without practically altering the energy of the triplet level the small admixture to it of the D state will lead to a qualitatively new result: to the appearance in the system of a quadrupole moment Q[2] (cf., with the analogous mechanism for the appearance of a quadrupole moment in a deuteron[4]; we also note